Journal Pre-proof

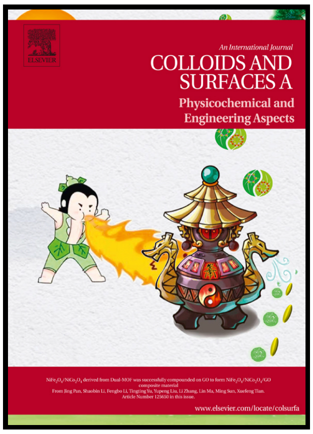

Application of Mesoporous Silica Particles as an Additive for Controlling Rheological, Thermal, and Filtration Properties of Water-Based Fluids

Federico Fookes, Yurany Villada, María Eugenia Taverna, Carlos Busatto, Juan Maffi, Natalia Casis, Camilo Franco Ariza, Farid Cortes, Diana Estenoz

PII: S0927-7757(24)01567-X

DOI: https://doi.org/10.1016/j.colsurfa.2024.134703

Reference: COLSUA134703

To appear in: *Colloids and Surfaces A: Physicochemical and Engineering Aspects*

Received date: 27 December 2023
Revised date: 4 April 2024
Accepted date: 2 July 2024

Please cite this article as: Federico Fookes, Yurany Villada, María Eugenia Taverna, Carlos Busatto, Juan Maffi, Natalia Casis, Camilo Franco Ariza, Farid Cortes and Diana Estenoz, Application of Mesoporous Silica Particles as an Additive for Controlling Rheological, Thermal, and Filtration Properties of Water-Based Fluids, *Colloids and Surfaces A: Physicochemical and Engineering Aspects,* (2024) doi:https://doi.org/10.1016/j.colsurfa.2024.134703

Application of Mesoporous Silica Particles as an Additive for Controlling Rheological, Thermal, and Filtration Properties of Water-Based Fluids

Federico Fookes[a], Yurany Villada[b], María Eugenia Taverna[a,c,d], Carlos Busatto[a], Juan Maffi[e], Natalia Casis[a], Camilo Franco Ariza[b], Farid Cortes[b], Diana Estenoz[a,d,*]

[a]INTEC (Universidad Nacional del Litoral – Conicet). Güemes 3450, (3000) Santa Fe, Argentina

[b]Grupo de Investigación Fenómenos de Superficie-Michael Polanyi, Departamento de Procesos y Energía, Facultad de Minas, Universidad Nacional de Colombia, Medellin, Colombia

[c]UTN Facultad Regional San Francisco, Av. de la Universidad 501, (2400) San Francisco, Argentina

[d]Facultad de Ingeniería Química, Santiago del Estero 2829, (3000) Santa Fe, Argentina

[e]Departamento de Movilidad y Ambiente, Instituto Tecnológico de Buenos Aires (ITBA), Lavardén 315, C1437FBG Buenos Aires, Argentina

*Diana Estenoz (destenoz@santafe-conicet.gov.ar)

Abstract

Mesoporous silica particles (MSP) have received increasing interest for various applications because of their unique features such as controlled pore size, low density, high chemical and thermal stability, and high surface area. In this study, MSP was applied as an additive in water-based drilling fluids (WBMs). The effect of MSP on the rheological, thermal, filtration, and structural properties of WBMs was investigated. The results were compared with those of analogous fluids containing conventional nonporous silica particles (SSP). Rheological assays showed shear-thinning and viscoelastic behavior, which were more noticeable for fluids including MSP. It was observed that low concentrations of MSP (0.25%wt) can achieve the same rheological properties as the fluids with higher SSP content (up to 0.5%wt). The rheological properties of SSP-containing fluids were not significantly affected by the presence of NaCl or aging tests. The theoretical Herschel–Bulkley model represents the rheological behavior of WBMs. The MSP-based WBMs exhibited better filtration properties before aging. The microstructures of the WBMs were analyzed using Scanning Electron Microscopy (SEM). A homogeneous distribution of SSP in the WBMs was observed, while particle agglomeration was observed in WBMs containing MSP. In addition, surface interactions were studied to elucidate the interactions between particles and fluid constituents. The surface interaction, assessed through ζ-potential and FTIR analysis, revealed that the binding affinities of BT, PAC, and XGD with MSP were augmented compared to their individual values. Based on the experimental results, MSP constitutes a promising alternative as an additive for the design of WBMs.

Graphical abstract

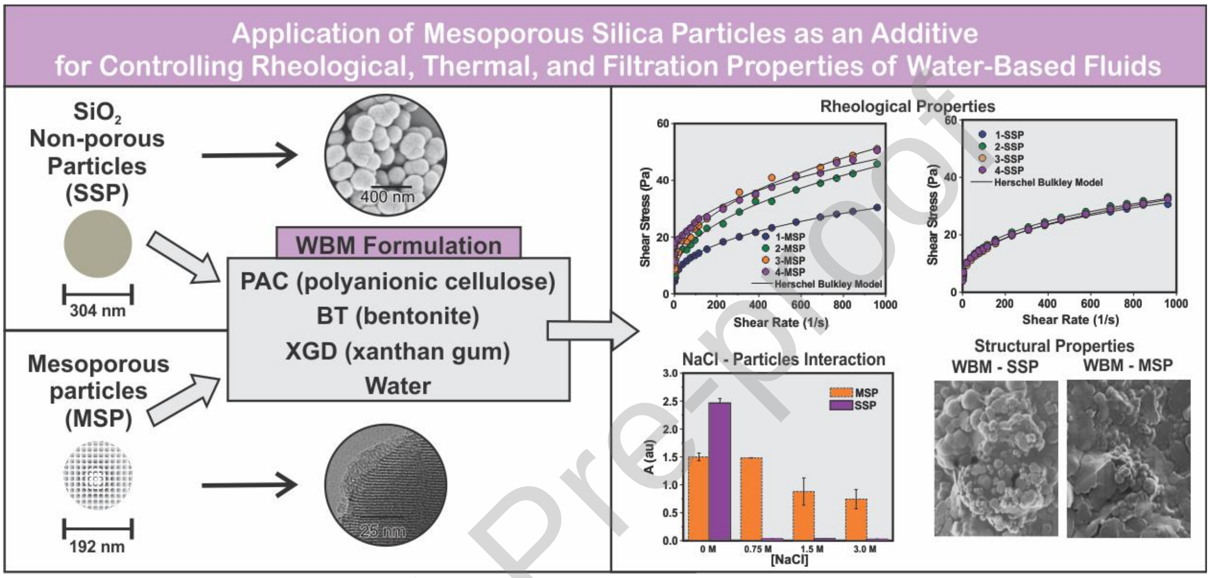

***Keywords*:**

drilling fluids, mesoporous silica particles, silica particles, rheology, surface interactions.

Abbreviations

WBMs, water-based drilling fluids; MSP, mesoporous silica particles; SSP, nonporous silica particles; OBMs, oil-based drilling fluids; TEOS, tetraethoxysilane; CTAB, cetyltrimethylammonium bromide; NaCl, sodium chloride; BT, bentonite; PAC, polyanionic cellulose; XGD, xanthan gum; MMT, montmorillonite; SEM, scanning electron microscopy; DLS, dynamic light scattering; TEM, transmission electron microscopy; FTIR, Fourier-transform infrared spectroscopy; BET, Brunauer-Emmett-Teller; GS, Gel strength (Pa); PV, Bingham plastic viscosity (cP); YP, Bingham yield point (Pa).

Introduction

Global energy demand is increasing owing to industrial activity and technological advances in both developing and developed countries (Karakosta et al., 2021). Therefore, the exploration and design of novel sustainable technologies for hydrocarbon exploitation represent attractive alternatives (Afolabi, 2019). Drilling fluids are employed in the oil and gas drilling industry, providing several functions such as removing drilled cuttings, lubricating, and cooling the drill bit and providing hydrostatic pressure to maintain borehole stability, among others (Ali et al., 2022; Novara et al., 2021). The fulfillment of these features is based on the lithology of the drilled formation and the properties of the drilling fluid, which should be designed to achieve the required performance (Gautam et al., 2022). Drilling fluids are mixtures of solids and liquids dispersed or dissolved in the water or oil phase. Depending on their composition, drilling fluids can be classified as water-based drilling fluids (WBMs) and oil-based drilling fluids (OBMs). WBMs present several advantages over OBMs because of their low cost, superior cooling and cutting removal ability, rapid formation penetration rate, and low environmental footprint (H. M. Ahmad et al., 2021).

Different additives are typically added to WBMs to improve their performance. Synthetic and natural polymers are the most common materials used to enhance rheological and filtration properties and mitigate wellbore instability issues. However, with an increase in well depth and higher bottom hole temperatures, the thermal stability of polymer additives becomes a significant property (Al-Yasiri et al., 2019). Recently, the dispersion of particles in drilling fluids has been proposed as a potential alternative to improve drilling fluid performance, particularly under downhole conditions (Rafati et al., 2018).

Particles based on ***hybrid systems*** (titanium oxide/polyacrylamide, silica oxide/acrylic resin, zinc oxide/acrylamide, polyethylene glycol/silica, clay nanoparticles with poly (styrene/co-methyl methacrylate), ***ceramic nanoparticles*** (silica, zinc oxide, titanium dioxide, cupric oxide, clay particles) (Aftab et al., 2017; Vryzas & Kelessidis, 2017), ***metal nanoparticles*** (iron, calcium, zirconium, silver, zinc) (Rafati et al., 2018), ***carbon-based nanoparticles*** (fullerenes and carbon nanotubes), (Cheraghian, 2021; Ikram et al., 2021) and nanoparticles ***based on natural polymers*** (nanocrystalline and nanofibrillar cellulose and chitin nanocrystals) (M.-C. Li et al., 2018; Villada et al., 2018) have been investigated as additives for WBMs. Silica particles are one of the most studied additives in WBMs because of their attractive properties such as high surface-to-volume ratio, controlled size and morphology, and surface characteristics that promote the reduction of water invasion in shale and the control of rheology and filtration properties, among others(Fakoya & Shah, 2017). Silica particles can be synthesized using several methods, including sol–gel, plasma, and microwave irradiation methods (Mirzaasadi et al., 2021), and the sol-gel technique is the most employed. Numerous studies have shown that silica nanoparticles significantly affect the rheological properties of WBMs (Esfandyari Bayat et al., 2021; Rafati et al., 2018). Salih et al. (2016) concluded that silica nanoparticles improved the hydraulic, rheological, and filtration properties of water-based muds with low concentrations (Salih et al., 2016). Liu et al. (2016) (Liu et al., 2016) studied the effect of silica nanoparticles on the performance of WBMs. The authors argued that silica particles could improve the cutting transportation rate by increasing the colloidal force between the cutting and particles (Kök & Bal, 2019; Porgham Daryasari et al., 2019).

Porous silica has received much attention in recent years owing to its unique features, such as controlled pore size and morphology, low density, high chemical and thermal stability, and high surface area (Islam & Nebhani, 2021). In particular, mesoporous silica particles (MSP) have been studied for several applications such as polishing, chromatography, catalysis, drug delivery, and medical implants (Khalil et al., 2020; Narayan et al., 2018; Vallet-Regí, 2022). Recently, the potential use of MSP as an additive in water-based drilling fluids was investigated (Bardhan et al., 2024; Zarei et al., 2023). The experimental results indicated that MSP can significantly enhance the thermal properties of water-based drilling fluids, maintain rheological characteristics, greatly reduce fluid loss, and provide some inhibitive properties. However, although MSP showed promise as additives in drilling fluids, their performance compared to silica nanoparticles has not been thoroughly studied. Additionally, a study examining the interactions between SSP or MSP and the fluid components in the presence of salt was not conducted.

In this study, silica particles with different morphologies (MSP and SSP) were synthesized and characterized. Particles were dispersed in water and used to prepare WBMs. The effect of particle addition on the rheological, filtration, structural, and thermal properties of the WBMs was investigated. The properties of fluids containing MSP were assessed and compared to those of fluids containing conventional SSP. The study was complemented with surface interaction studies using ζ-potential and FTIR analysis to elucidate the contribution of the silica particle morphology to the functional properties of fluids.

Materials and methods

Materials

Tetraethoxysilane (TEOS) (Fluka, Seelze, Alemania), cetyl trimethylammonium bromide (CTAB) (Sigma-Aldrich, St. Louis, MO, USA), sodium hydroxide, ammonia solution, sodium chloride (NaCl), and ethanol (Cicarelli, Argentina) were purchased and used without further purification. Bentonite (BT) was obtained from MARBAR S.R.L. Xanthan gum (XGD) and polyanionic cellulose (PAC) was provided by MI-Sawco. They exhibit average molecular weights of 1.62×106 and 1.13×106 g/mol, respectively, as it was previously reported (Villada et al., 2017). Deionized water was used to prepare all the WBMs. All additives were used as received.

Synthesis of silica particles (SSP)

SSPs were synthesized according to a modified Stöber method(Kadhem et al., 2018). First, 22 mL of ammonia solution 25 %, and 200 mL of ethanol 96% were mixed in a round bottom flask and stirred at 300 rpm for 20 min. TEOS (14 mL) was then quickly added, and the flask was tightly sealed. The obtained mixture was allowed to react at room temperature under stirring for 12 h. The obtained particles were centrifuged at 10,000 rpm for 7 min and redispersed five times in distilled water to eliminate the remaining reactants.

Synthesis of mesoporous silica particles (MSP)

MCM-41 type MSPs were synthesized following the procedure reported by Williams et al. (2015) (Williams et al., 2015). Briefly, 2.2 mmol of CTAB (800 mg) and 2.8 mL of 2 M NaOH water solution were mixed with 21 mol of water (384 mL). When the solution became homogeneous, 18 mmol (4 mL) TEOS was added dropwise. Then, the resulting mixture was stirred at 80 °C for 2 h. The resulting solution was maintained at room temperature for 1 h and the particles were filtered, washed with deionized water, and dried at 60 °C. Finally, the particles were calcined for 4 h at 550 °C to remove any remaining surfactants.

Characterization of particles

i) Dynamic light scattering (DLS)

Particle size was analyzed by DLS using a BI-200SM instrument (Brookhaven). The measurements were performed at detection angles of 90° °C and 30 ° °C. Appropriate dilution of the samples was carried out with filtered ultrapure water to minimize the noise-to-signal ratio.

ii) Scanning electron microscopy (SEM)

The morphology of the silica particles was investigated by SEM. The samples were placed over an aluminum stub and sputter-coated with gold at 40 mA for 90 s using a Balzer SCD 030 sputter coater. The samples were analyzed using a ZEISS FE-SEM Σigma microscope (Jena, Germany) at an acceleration voltage of 3 kV. The average particle size was determined using image processing software (ImageJ, National Institutes of Health, Bethesda, Maryland, USA) after analyzing approximately 300 particles per sample.

iii) Transmission electron microscopy (TEM)

The porous structure of the MSP was studied using TEM. The samples were placed on a carbon-coated copper grid, air-dried, and observed at an accelerating voltage of 200 kV using a JEOL-2100 Plus electron microscope (JEOL, Tokyo, Japan).

iv) Surface area and porosity of MSP

The textural properties of the particles were evaluated using nitrogen sorption analysis on a Micromeritics ASAP 2020 Plus sorptometer. The samples were then degassed at 100 °C for 12 h. The surface area and mean pore diameter were calculated using the Brunauer-Emmett-Teller (BET) and Barrett-Joyner-Halenda (BJH) models, respectively. The total pore volume was estimated as $p/p_o = 0.99$. The micropore volume and the specific surface area of the mesopores were calculated with the t-plot method in the $3.5 \text{ Å} < t < 5.0 \text{ Å}$ range.

Formulation of WBMs

Water-based muds were prepared based on the Recommended Practice for Field Testing Water-based Drilling Fluids (API RP 13B-1, American Petroleum Institute, 2009). Na-BT was used as the primary viscosifier and XGD was used as a rheological modifier. Low-viscosity PAC (PAC-LV) was used as a filtration control additive.

Several WBMs containing silica particles (SSP or MSP), BT (1%wt), XGD (0.5%wt), PAC (0.5%wt), and H_2O were prepared. Eight WBMs were evaluated varying the concentration of both silica particles: 0% (1-MSP or 1-SSP), 0.25% (2-MSP or 2-SSP), 0.50% (3-MSP or 3-SSP), and 0.75% (4-MSP or 4-SSP). The pH and density of the prepared fluids are in the range of 9 ± 0.5 and 1.50 g/cm^3, respectively. Table 1 lists the compositions and relevant characteristics of these fluids. To investigate the interaction of NaCl with fluid components, two assays were performed. Initially, 3-SSP and 3-MSP fluids were formulated with a sodium chloride concentration of 0.75 M, and their rheological behavior was evaluated. Additionally, suspensions of particles in different NaCl media (0, 0.75, 1.5, and 3 M) were prepared and the absorbance was measured.

Table 1. Formulation and characteristics of SSP and MSP groups of WBMs (without aging and salt effect).

	Fluid	**BT (%wt)**	**XGD (%wt)**	**PAC (%wt)**	**SSP or MSP (%wt)**	**PV (cP)**	**YP (Pa)**	**GS (Pa)**		**Filtrate volume at 30 min**	**Filter cake thickness (mm)**
								10 min	**30 min**		
SSP Group	**1-SSP**	1.0	0.5	0.5	0.00	13.39	18	18	21	16.8	1.5
	2-SSP	1.0	0.5	0.5	0.25	13.21	21	18	21	16.4	1.4
	3-SSP	1.0	0.5	0.5	0.50	13.84	19	19	22	13.8	1.3
	4-SSP	1.0	0.5	0.5	0.75	13.21	20	19	22	15.9	1.3
MSP Group	**1-MSP**	1.0	0.5	0.5	0.00	13.39	18	18	21	16.8	1.5
	2-MSP	1.0	0.5	0.5	0.25	23.60	23	19	21	8.3	1.2

3-MSP	1.0	0.5	0.5	0.50	24.71	28	20	22	8.1	1.1
4-MSP	1.0	0.5	0.5	0.75	25.07	26	21	23	8.0	1.1

Characterizations of WBMs

Steady and dynamic rheological properties

Steady-state viscosity was measured using a viscometer (Brookfield) at various shear rates. The apparent viscosity and shear stress were measured as functions of shear rate, ranging from 30 to 1000 s^{-1}. All measurements were conducted at 25°C and repeated three times.

Dynamic measurements were carried out in a Haake RheoStress RS80 rheometer (Haake Instruments Inc., Paramus, 219 NJ, USA) with a cone-plate geometry (60-mm diameter, 1° angle). The linear viscoelastic region was determined by strain sweep tests from 0.01 0.10 Hz. Frequency sweep tests were performed from 0.01 to 10 Hz within the linear viscoelastic region at strains of 0.02, and room temperature. This assay was repeated twice. To predict the theoretical rheological performance of WBMs, conventional non-Newtonian rheological models, such as the power law, Sisko Model, and Herschel-Bulkley model, were fitted to the results of the rheological assays (Villada et al., 2017). Additionally, the gel strength, yield point, and plastic viscosity were determined using the viscosimeter Fann 35 (USA) and the methodology reported by Novara et al, 2021 (Novara et al., 2021).

Structural characterization of WBMs

The structure of the WBMs was investigated using scanning electron microscopy (SEM). The fluids were placed over an aluminum stub and sputter-coated with gold at 40 mA for 90 s using a Balzer SCD 030 sputter coater. The micrographs were acquired employing the methodology used to study the morphology of silica particles.

Thermal properties of WBMs

The Dynamic aging tests were conducted using a roller oven OFITE (Houston, TX, USA) at 90°C and 120 ºC for 960 min. After aging, rheological properties were evaluated using a previously described procedure. The WBMs were compared before and after aging.

Filtration properties

Water from WBMs is transported through the nanopores of shale and can cause wellbore instability. Therefore, low filtrate volumes of WBMs can decrease wellbore instability risk (Edalatfar et al., 2021). Static fluid loss was tested using a filter press (API filter press). To this effect, the fluid was placed in a stainless-steel chamber with an opening at the bottom, and the filter paper was a G50 Whatman quantitative filter paper (9 mm diameter, 2.7 μm pore size). The flow was started at a pressure of 100 psi and the volume of fluid was recorded as a function of time (30 min) at room temperature. Furthermore, the permeability of the filter cakes was determined following Darcy's law (Villada et al., 2020).

Surface interaction studies

The surface interactions between particles and WBM additives were investigated using the ζ-potential and FTIR analysis. ζ-potential measurements were carried out using a Zetasizer Nanoseries Malverl (ZS90) for the analysis of suspensions of BT, XGD, PAC, particles, and blends of BT-MSP, BT-SSP, PAC-SSP, PAC-MSP, XGD-SSP, and XGD-MSP (1 g L^{-1}) prepared in deionized water and sonicated for 10 min. The reactive ratio was selected based on the WBM formulation. A drop of each suspension was then added to the KBr discs. FTIR analysis was performed on a Shimadzu Model 8201 Fourier transform spectrophotometer in the frequency region 4000–500 cm^{-1} at 40 scans.

Results and discussion

Characterization of particles

Silica particles were synthesized by the sol-gel method as described previously; its properties are listed in Table 2 From DLS analysis, which shows that MSP exhibited a larger particle size than SSP (304 ± 35 and 192 ± 17 nm, respectively). Differences in particle size can be observed in the SEM micrographs (Figure 1a and b). SEM observations showed a spherical morphology for SSP and a round morphology for MSP, with particle size values in agreement with the results obtained by DLS measurements. The morphology and porous structure of the MSP were also examined by TEM (Figure 1c). TEM micrographs revealed a highly ordered pore network in the MSP. Similar results were reported by Cai et al. (2001)(Cai et al., 2001). An average pore diameter of approximately 2 nm was observed using TEM.

The ζ-potential values indicate a more negative surface charge for SSP compared to that of MSP particles (-55.6 ± 2.1 and -23.9 ± 2.7 mV, respectively). This difference could be attributed to the reduction of hydroxyl groups of MSP due to the condensation of silanol groups to form siloxane bonds during the calcination step (Cao et al., 2016). However, MSP exhibited a value close to -25 mV indicating colloidal stability (Shnoudeh et al., 2019). Table 2 summarizes the main characteristics of the particles. SSP exhibited a Type IV adsorption isotherm, with a BET surface area of 14 m^2/g. In contrast, MSP showed a surface area of 1143 m^2/g and a narrow pore size distribution of 2.87 nm, which is typical of mesoporous materials (Fookes et al., 2022).

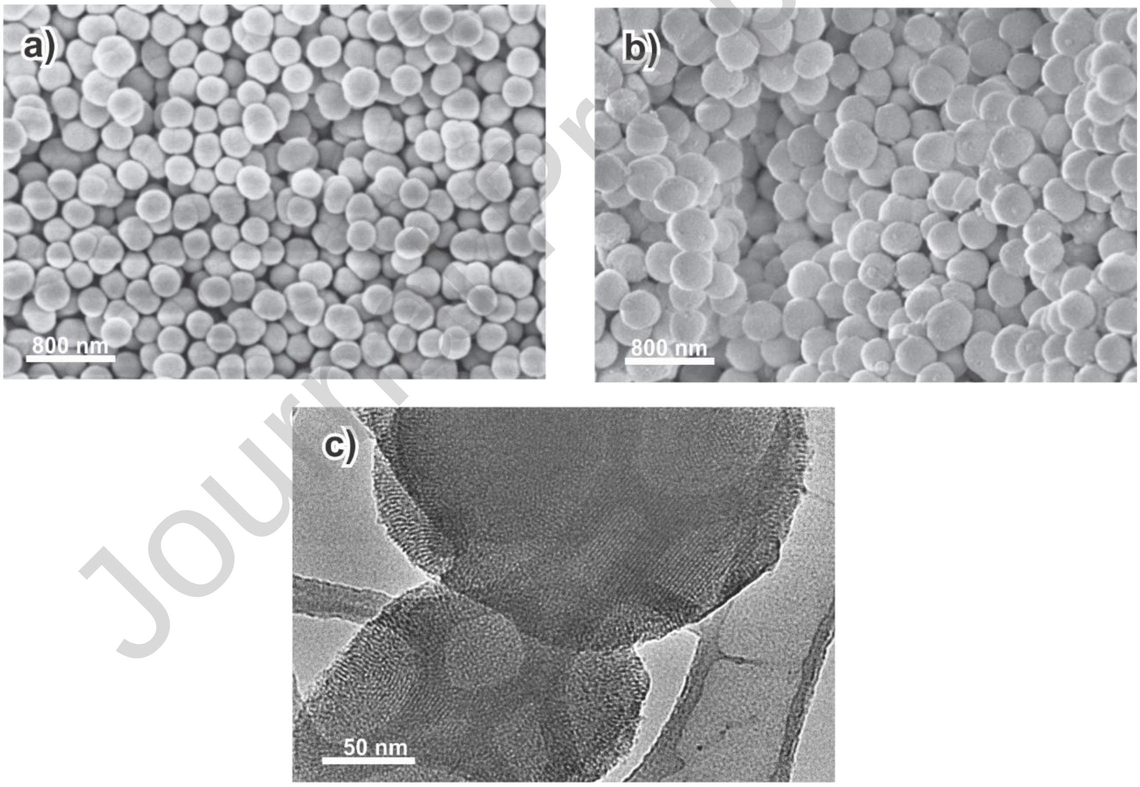

Figure 1. Characterization of silica particles by SEM and TEM: a) SEM micrographs of SSP; b) SEM micrographs of MSP; c) TEM micrographs of MSP.

Table 2. Size, surface charge, and textural properties of SSP and MSP particles.

Property	**Unit**	**SSP**	**MSP**
Diameter	(nm)	304 ± 35	192 ± 17

ζ-potential	(mV)	-55.6 ± 2.1	-23.9 ± 2.7
BET specific surface area	(m^2/g)	14	1143
Pore size	(nm)	-	2.87

WBMs characterizations

Rheological properties

Bentonite is a montmorillonite clay commonly used in WBMs as a viscosifier and filtration control agent. BT is mostly composed of montmorillonite (MMT) platelets. BT platelets maintain permanent negatively charged faces owing to the isomorphic substitution of the lattice cations. In contrast, the surface charges on the edges of the BT platelets were pH dependent (Luckham & Rossi, 1999). Platelet edges can be positively or negatively charged under acidic or alkaline conditions, respectively. BT platelets can be associated through three modes (face-face, edge-face, and edge-edge) in aqueous suspensions as a result of van der Waals forces, hydrogen bonds, electrostatic repulsion forces, and electrostatic attraction forces (Lavoine et al., 2012; M. Li et al., 2020). Owing to the alkaline pH of the prepared WBMs, BT was negatively charged (-31.7 mV) on its face and edge.

Xanthan gum and polyanionic cellulose are anionic branched and linear biopolymers, respectively. They are negatively charged due to the presence of carboxylic groups (-11.8 mV and -34.4 mV).

Figure 2 presents the rheograms of the WBMs containing different concentrations of silica particles. Shear-thinning behavior was observed for all the WBMs. In addition, fluids containing SSP (**SSP group**) exhibited lower viscosity values than those formulated with MSP (**MSP group**) (Figure 2a and b). It was also observed that the viscosity increased with increasing concentration of MSP particles. In contrast, the effect of the SSP concentration was not as noticeable as previously observed (Aramendiz & Imqam, 2019; Bayat & Shams, 2019). On the other hand, SSP exhibit a more negative charge, which could promote repulsion with other additives. This behavior could be associated with the lower viscosities of the fluids containing SSP. In addition, the viscosity of fluids can be strongly determined by the differences in the surface characteristics of particles and surface interactions between the additives.

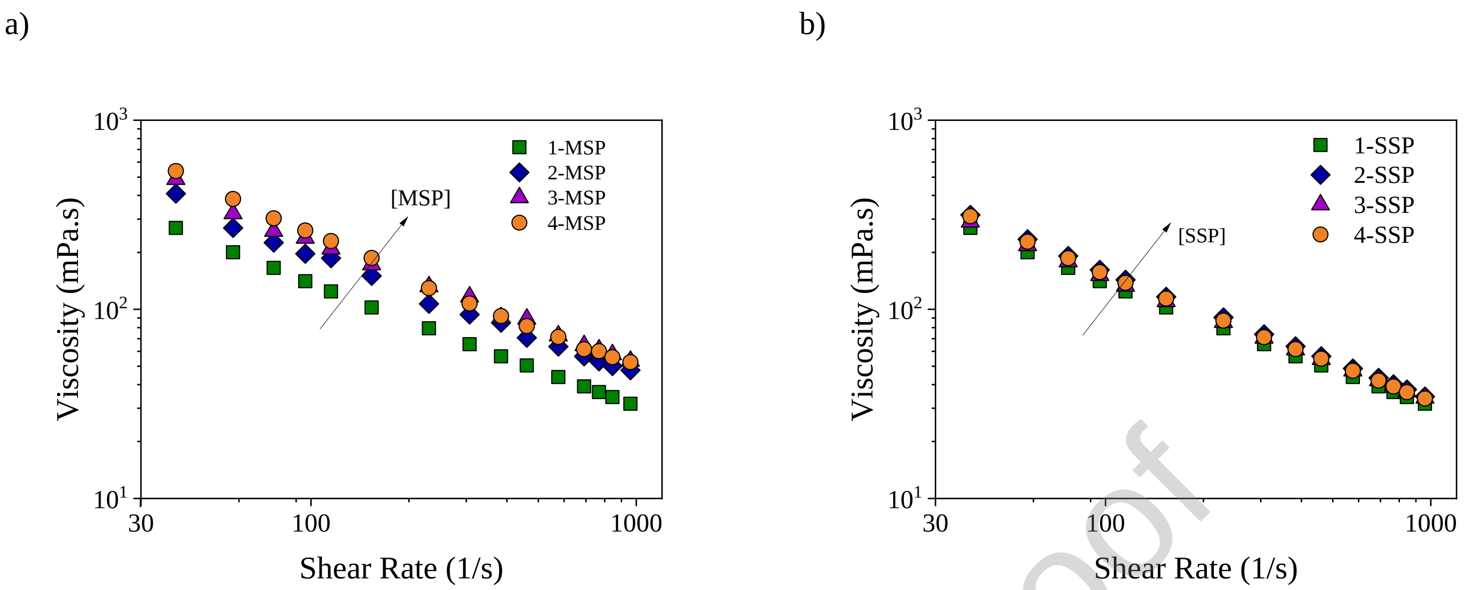

Figure 2. Effect of particle type and content in the rheological properties of WBMs: a) SSP, b) MSP particles

Liu et al. (2016) (Liu et al., 2016) observed that the high specific surface area of porous silica particles may provide more area for interaction with the polymer chains, which leads to an improved shear thickening effect.

However, the distribution of particles is different for fluids. WBMs formulated with MSP present a more compact structure with aggregates or hydroclusters of MSP that promote an increase in viscosity. In addition, the WBMs were formulated under alkaline conditions, and the SSP and polymers exhibited strong negative ζ-potential values that led to greater electrostatic repulsion, preventing the particles from agglomerating (William et al., 2014). Likewise, the low tendency of BT clay to form stacks in the presence of particles promotes a much looser structure with poor rheological properties, which agrees with the SEM micrographs presented in Figure 3.

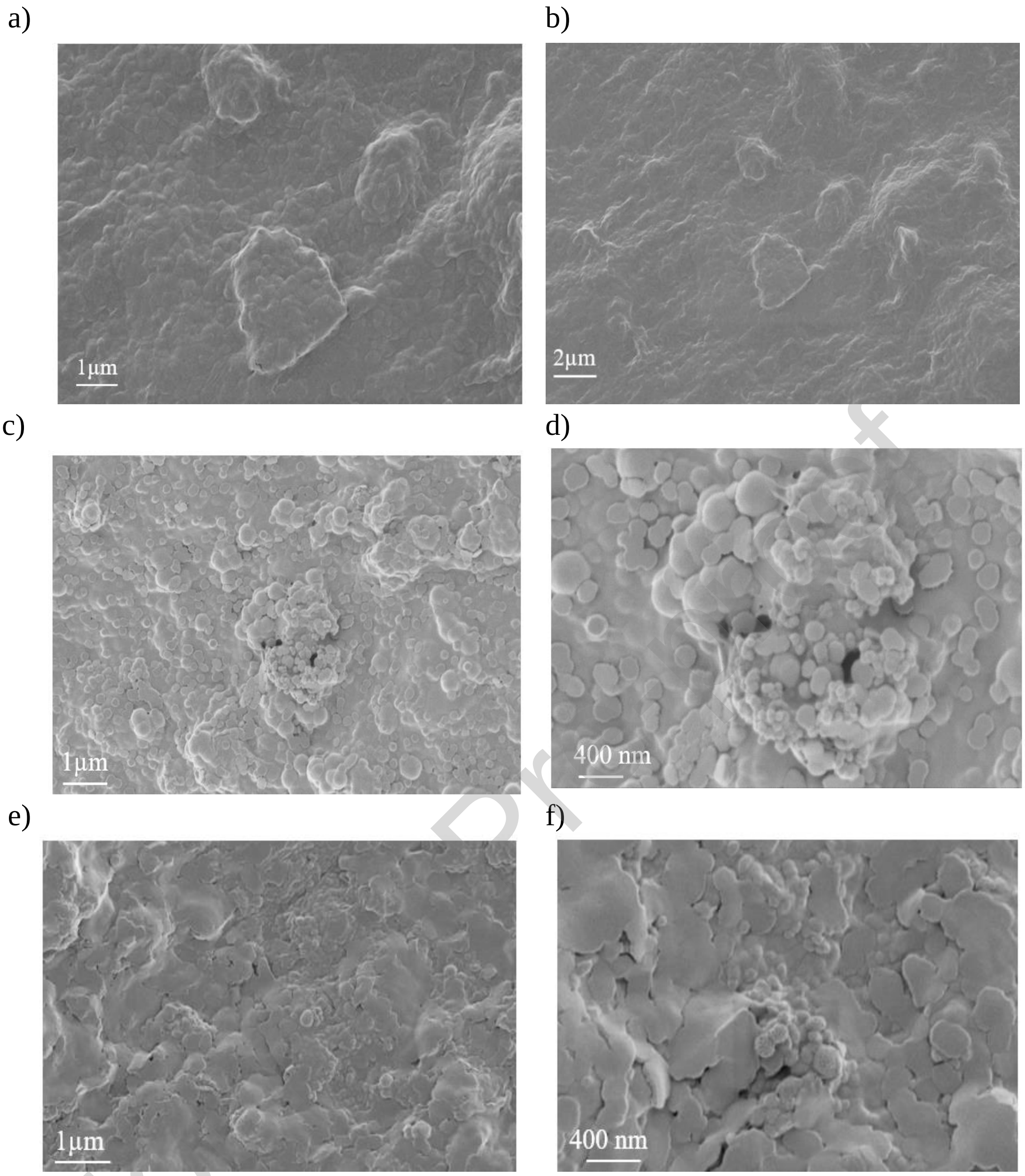

Figure 3. SEM micrographs of: a, b) BT suspension (1 and 2 μm), c,d) WBM containing SSP (1 μm and 400 nm) , and e,f) WBM with MSP particles (1 μm and 400 nm).

The plastic viscosity (PV), yield point (YP), and gel strength (GS) of the studied WBMs are presented in Table 1. It can be observed that the PV, YP, and GS for the fluid containing SSP slightly increased with increasing particle concentration. In contrast, the PV, YP, and GS values of the MSP-based fluids increased with increasing particle concentration. Again, these parameters confirmed the greater viscosifying effect of MSP particles.

Overall, the complex microstructure of multicomponent systems (clay, silica particles, and XGD and PAC polymers) is mainly determined by the association mode of clay, surface charge and structures of silica particles, and molecular properties of XGD and PAC.

However, MSP have a high surface area compared to non-porous particles, which could be the main factor determining the rheological properties of WBMs. Note that lower concentrations of MSP (0.25%wt) are required to achieve the same rheological properties as the fluids containing SSP.

Figure 4 shows the mechanical spectra of the 3-SSP and 3-MSP fluids. The WBMs exhibited viscoelastic behavior, which was more noticeable for WBMs containing MSP.

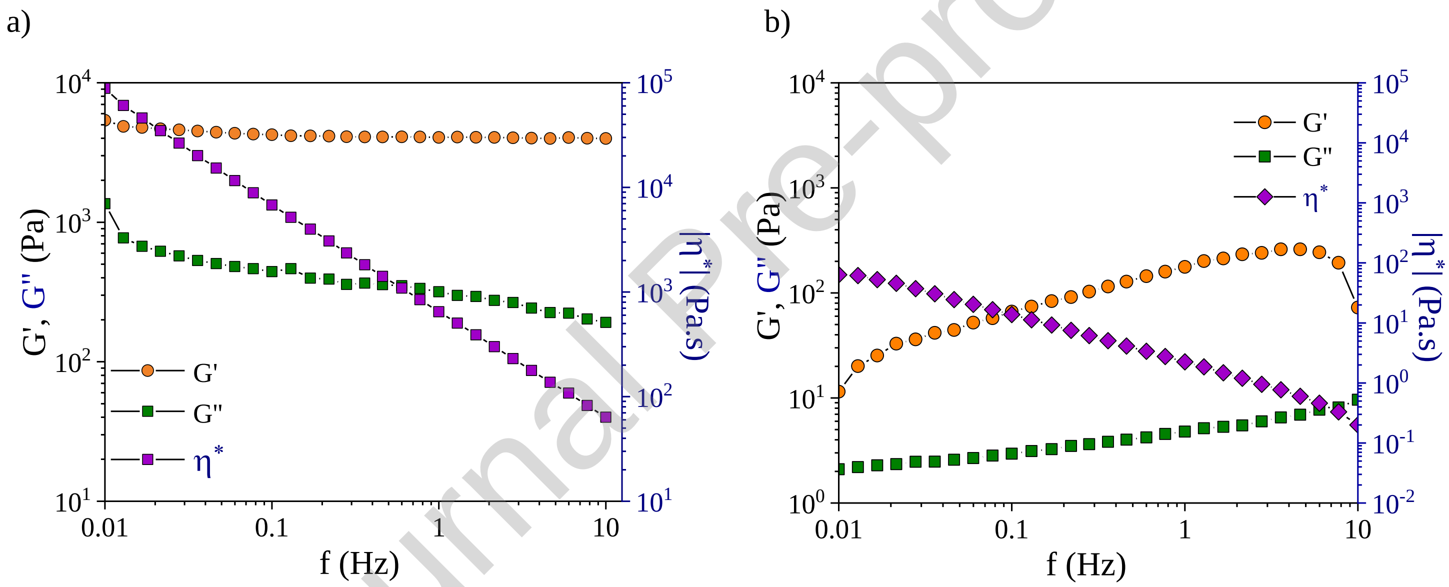

Figure 4. Mechanical spectra of the effect of particles type in the rheological properties of WBMs: a) 3-MSP, and b) 3-SSP.

Finally, rheological models were used to theoretically predict the behavior of drilling fluids. Three rheological models (Power Law, Sisko, and Herschel Bulkley) were employed to evaluate the rheological behavior of the WBMs. The power Law and Sisko parameters are presented in Supplementary Information (SI). Figure 5 shows the curve of the experimental shear stress as a function of shear rate for WBMs, as well as the Herschel–Bulkley model predictions. It can be observed that the Herschel Buckley model provides a good overall fit of the experimental data. The parameters of the Herschel–Bulkley model, RSMD, and R^2 are listed in Table 3. As expected, the yield point (τ_0)

increases with increasing silica particle concentration. On the other hand, a trend of the flow consistency coefficient (k') is not observed due to the low accuracy in this range of shear rate. This effect is more significant for the WBMs corresponding to MSP group. Likewise, the flow behavior index (n') is lower than 1, indicating a shear thinning behaviour of WBMs.

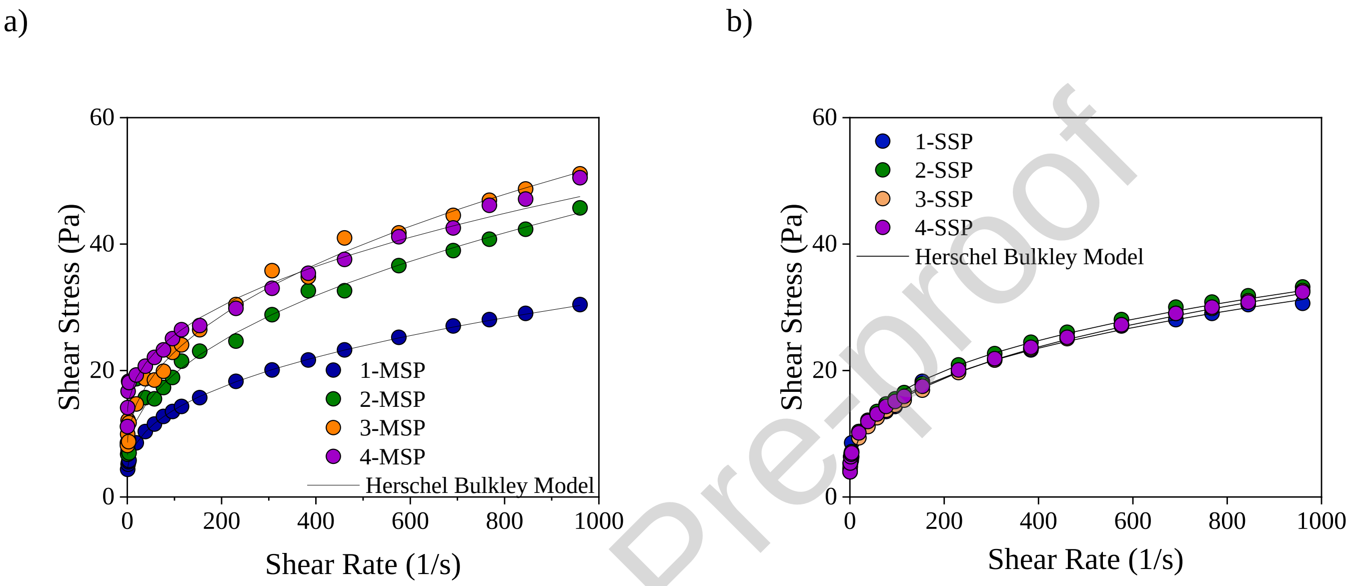

Figure 5. Effect of the particle concentration on the rheological behavior: a) MSP and b) SSP. Solid lines represent the Herschel-Bulkley model adjusted.

Table 3. Results for the parameter of rheological models adjusted.

Group	Fluid	MSP or SSP (%wt)	τ_0 (Pa)	k'' (Pa.s)	n''	RSMD	R^2
MSP	1-MSP	0.00	2.26	1.97	0.39	0.06	0.99
	2-MSP	0.25	5.57	1.66	0.46	1.27	0.98
	3-MSP	0.50	7.41	1.85	0.46	0.50	0.99
	4-MSP	0.75	12.23	1.87	0.43	0.59	0.98
SSP	1-SSP	0.00	2.26	1.97	0.39	0.06	0.99
	2-SSP	0.25	2.53	2.76	0.35	0.09	0.99
	3-SSP	0.50	2.72	2.09	0.39	0.04	0.99
	4-SSP	0.75	2.36	2.80	0.34	0.14	0.99

Effect of NaCl on the rheological properties

Sodium Chloride is the most common salt present during drilling. Several studies have confirmed that the presence of NaCl in fluids promotes flocculation, which affects their performance(Dankwa et al., 2018; Scheid et al., 2019). Sun et al. studied the influence of NaCl in the range of 0 to 6 M on the rheological properties of WBM. Although the specific viscosity, relative viscosity, and intrinsic viscosity were affected in the entire range, higher changes were observed from 0.2 to 0.8 M. In the current work, a 0.75 M concentration of NaCl was employed to compare the performance of MSP- and SSP-containing fluids(Sun et al., 2021). Figure 6 shows the effect of the NaCl concentration on the rheological properties of the 3-SSP and 3-MSP WBMs.

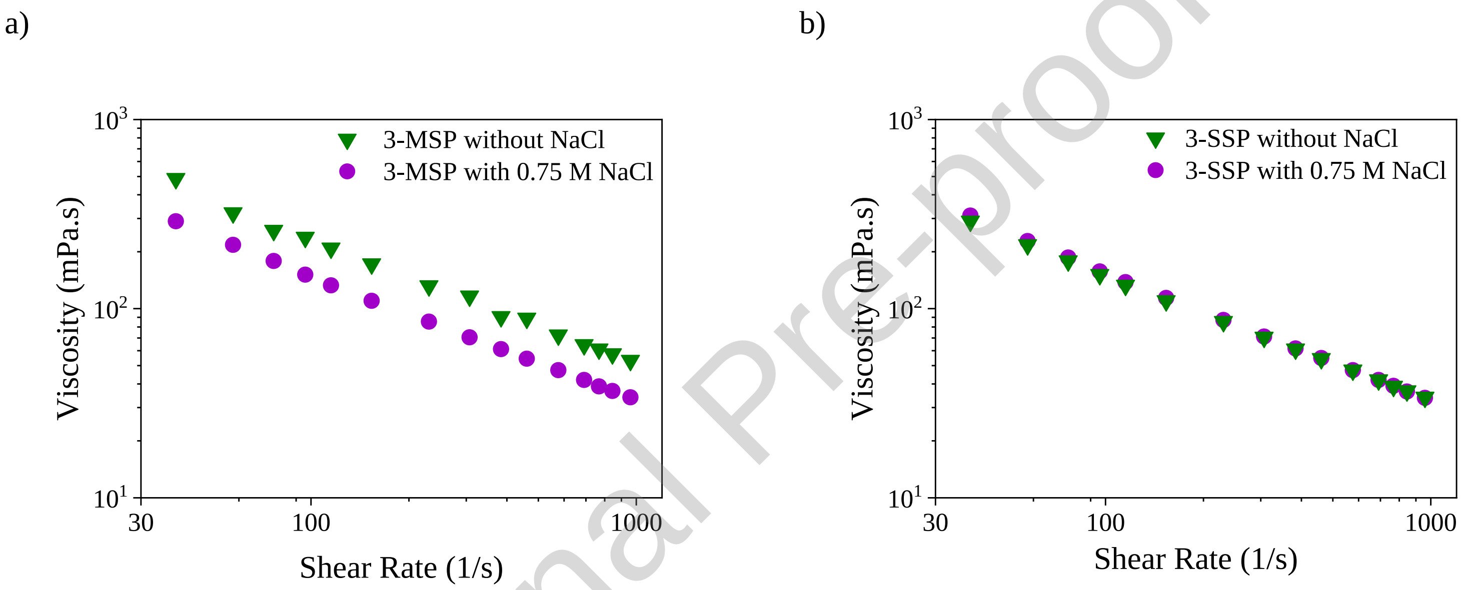

Figure 6. Effect of NaCl in the rheological properties of WBMs: a) 3-MSP and b) 3-SSP.

NaCl had a significant effect on the rheological behavior of WBMs containing MSP. In particular, viscosity decreased in the presence of NaCl. In contrast, the viscosity of the fluids containing SSP was not affected by the presence of NaCl. These results could be related to the compression of the diffuse double layer of BT. The negatively charged BT layers attract oppositely charged ions called counterions. The distance between the layers when the positive charges are in contact with water is referred to as the diffuse double layer(Lagaly, 1989). Owing to the higher surface charge, SSP presents high electrostatic attractions with NaCl, promoting an inhibition mechanism for the interaction between NaCl and BT. In particular, the particles were solvated with NaCl. Similarly, a repulsive effect between the solvated particles and BT can be generated. MSP has a lower surface charge than SSP, and this condition promotes a lower electrostatic attraction with NaCl and the possibility of NaCl interacting with BT, reducing the diffuse double layer. These observations were corroborated by UV-VIS assays. To this end, the absorbance of particle suspensions at several NaCl concentrations was measured. As shown in Figure 7, an increase in NaCl concentration produced a reduction in the absorbance values of the suspensions. This effect was more noticeable for SSP suspensions, indicating a stronger interaction between NaCl and SSP.

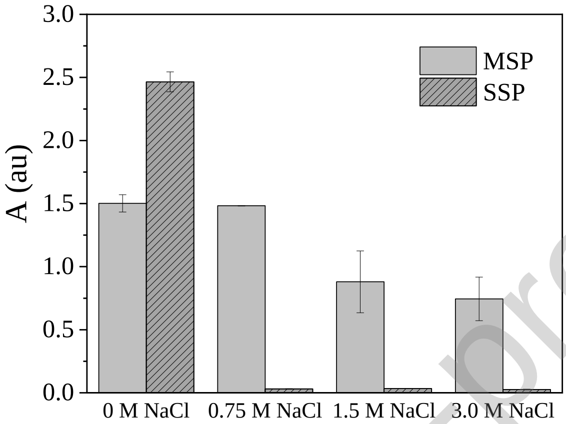

Figure 7. Effect of NaCl concentration on the absorbance of particles suspensions.

Thermal Stability

Figure 8 shows the rheological behavior of the WBMs after thermal treatment. Fluids containing SSPs exhibited greater stability than those containing MSPs. This behavior can be associated with the interactions via hydrogen bonding produced by XDG and PAC self-association (between -COOH groups), and XGD or PAC–silica non-porous particles (the hydroxide group of the -COOH and -OH groups) prevent the degradation of the system(Kennedy et al., 2015).

a) b)

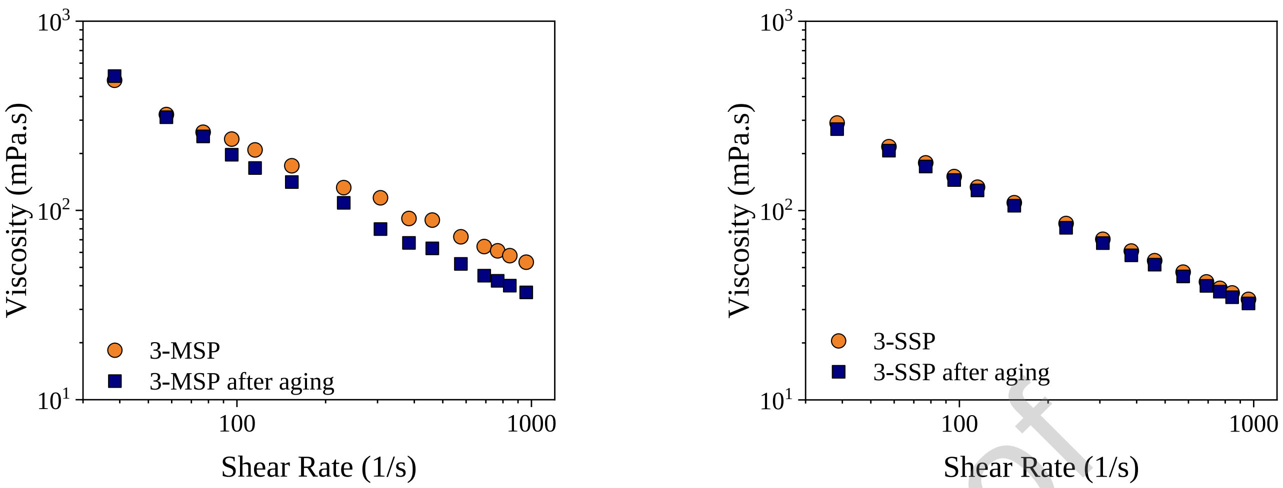

Figure 8. Thermal stability of WBMs: a) MSP, and b) SSP group.

Surface Interactions

The rheological properties of WBMs are mainly determined by several interaction mechanisms between clay (BT), polymers (XGD or PAC), and silica particles. The rheological behavior of WBMs has been extensively investigated and is related to the structural association (3-D network) of BT particles and other components. The BT association mode is dependent on the pH conditions, the presence of cations, and the types of ionic additives that affect the diffuse double layers surrounding the BT particles. In the case of binary particle-BT systems, BT platelets can be fully or partly intercalated or exfoliated, while particles can be fully dispersed or form large aggregates (Vryzas et al., 2019). These interactions have different effects on the flow behavior of the suspensions, affecting the rheological profile of the WBMs. The rheological properties of the studied multi-component system, BT, polymers, and silica particles (MSP and SSP) can be determined by BT particle interactions, BT-polymers, polymers-particles, and intermolecular interactions between them. Several authors have reported that interactions between BT and polymers can occur through different mechanisms, including electrostatic interactions, hydrogen bonding, and hydrophobic interactions. In general, the interactions between polymers and particles are based on the adsorption of particles onto the polymer structure through hydrogen bonding (Ibrahim et al., 2020). To study this mechanism in depth, the interactions between the WBMs components were studied by ζ -potential measurements and FTIR. All suspensions and blends were prepared with the same composition, as presented in the Methodology section. The ζ-potential values of the single components and BT-MSP, BT-SSP, PAC-MSP, PAC-SSP, XGD-MSP, and XGD-SSP blends are presented in Table 4. It was observed that the component suspensions and blends exhibited high negative charges, promoting the formation of stable blends. In addition, the blends containing SSP showed higher negative charges than the fluids containing MSP, indicating a high affinity for BT, PAC, and XGD. It is important to note that the ζ-potential of MSP aqueous suspensions is around -24 mV, rendering it unstable or near the value considered for stable suspensions of |-25 mV| (Shnoudeh et al., 2019). However, it is expected that in the fluids design that includes other additives (BT, XGD, and PAC), the values of ζ potential could be higher than |-25 mV|, ensuring the colloid stability required for the drilling operation.

Table 4. Results of ζ -potential for the additives and blends used in WBMs.

Component or Blend	ζ -potential (mV)	Standard Deviation
SSP	-55.6	2.08
MSP	-23.9	2.69
BT	-31.7	2.55
PAC	-11.8	3.63
XGD	-34.4	2.81
BT-SSP	-39.2	1.10
BT-MSP	-33.7	1.45
PAC- SSP	-61.3	2.88
PAC-MSP	-34.5	1.54
XGD-SSP	-38.0	2.25
XGD- MSP	-30.7	2.11

When analyzing the surface interactions of blends containing particles (MSP and SSP) and BT, it was observed that the ζ-potential values were more negative for SSP-BT. A similar effect was observed for the blends with particles and the XGD polymer. Although the values obtained from the interactions of BT and XDG with MSP were less negative than those of SSP, they were more negative than the initial values of MSP. This suggests an enhancement in the colloidal stability. Similarly, in the case of the blends with PAC and particles, the values of ζ-potential were more negative than those of the single components, suggesting a minor interaction for both particles.

It important

The FTIR spectra of BT, MSP, SSP, BT-MSP, and BT-SSP blends are shown in Figure 9. The following signals can be identified for BT clay: the peak of the Al–Al–OH stretching vibration at 3645 cm^{-1} is typical of smectites with a high amount of Al in the octahedral layer. The peaks at 3465 and 1656 cm^{-1} correspond to the H—O—H stretching and bending vibrations of the adsorbed water, respectively. The signal at 1047 cm^{-1} is attributed to the Si-O stretching frequency. Tetrahedral bending modes were observed for Si—O—Al at 530 cm^{-1} and for Si—O—Si at 470 cm^{-1} (Villada et al., 2017).

a) b)

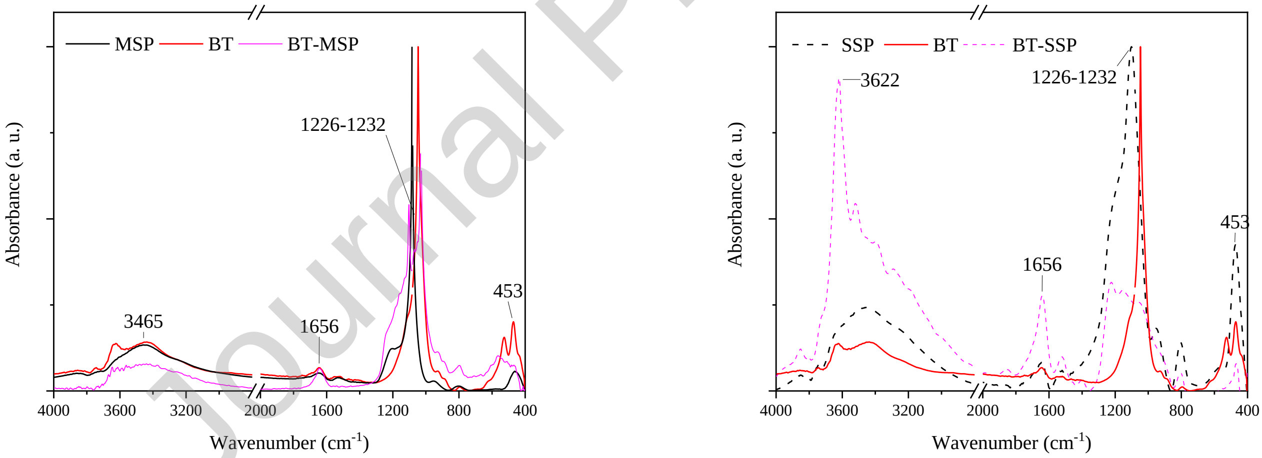

Figure 9. Surface interactions between BT clay and particles (MSP and SSP) through FITR. Spectra of MSP, BT, and BT-MSP blend (a), and SSP, BT, BT-SSP blend (b).

The FTIR spectrum of the SSP particles showed absorption bands of O–H stretching in H-bonded water at 3471 cm^{-1}. The peak at 1658 cm^{-1} is attributed to absorbed water molecules. The absorption bands between 800 and 1260 cm^{-1} were related to the superimposition of various SiO_2 peaks, Si–OH bonding, and peaks due to residual organic groups. The peaks at 1090 cm^{-1} and 960 cm^{-1} correspond to the asymmetric vibrations of Si–O and Si–OH, respectively. The symmetric vibration of Si–O is detected at 813 cm^{-1}. The band at 474 cm^{-1} represents the tetrahedral bending modes of Si-OH-Si (Beganskienė et al., 2014). Similar bands were observed in the MSP spectra. However, Yang et al. (2010) (Yang et al., 2010) assigned the absorption bands at 1232 cm^{-1} and 1226 cm^{-1} to the asymmetric stretching vibration of surface Si−O−Si groups, which are characteristic of mesoporous materials. Note that the peaks correspond to the signals of the BT-MSP and BT-SSP blends. Comparing the spectra of the BT-MSP and BT-SSP blends, it is observed that the bands at 3465, 1656, and 1226-1232 cm^{-1} present significant changes in the case of the SSP-BT blend. An increase in the band at 3622 cm^{-1} and 1656 cm^{-1} and a decrease in the bands at 1226-1232, and 453 cm^{-1}.

Figure 10 presents the FTIR spectra of PAC, MSP, SSP, and the blends of PAC-MSP and PAC-SSP. The peaks associated with the PAC polymer are 3452, 3152, 1629, 1423, and 1078 cm^{-1} corresponding to the O-H group stretching, stretching C-H bond, stretching of the carbonyl group (C=O), bending of bond C-H, and stretching of bond (C-O-C), respectively (M. Li et al., 2020). The bands in the MSP and SSP spectra are discussed above.

a) b)

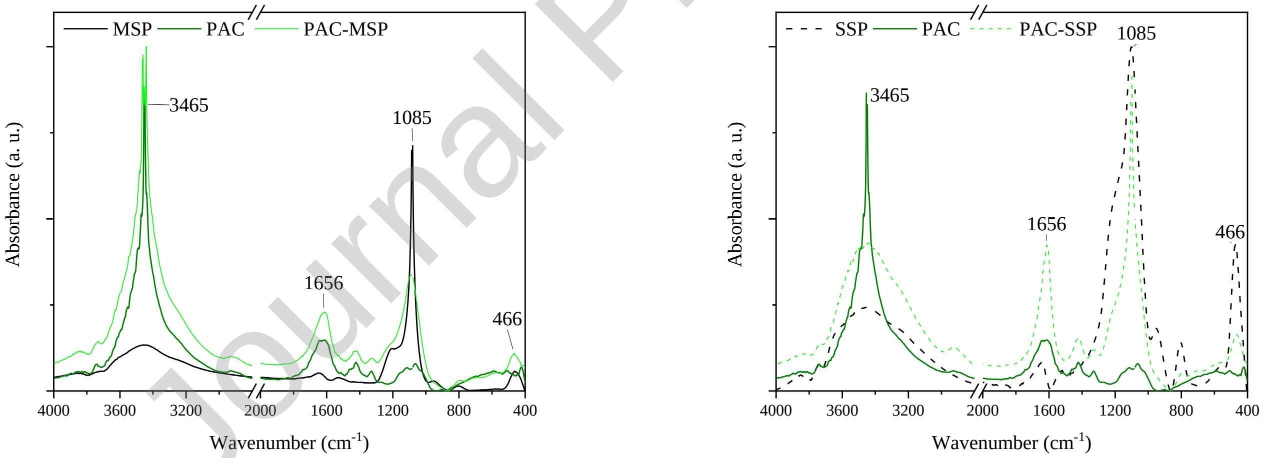

Figure 10. Surface interactions between PAC and particles (MSP and SSP) through FITR. Spectra of MSP, PAC, and PAC-MSP blend (a), and SSP, PAC, and PAC-SSP blend (b).

It can be observed that the bands of the blend spectra are like those of PAC. Significant changes were observed in the peaks of the spectra of the PAC-SSP blend. Specifically, increases in the bands at 3465 and 1656 cm^{-1} were observed concerning the SSP bands

(Figure 10b). In contrast, the intensity of the peak at 466 cm^{-1} decreased. This result was in accordance with the ζ -potential results.

The FTIR spectra of the XGD, MSP, SSP, XGD-MSP, and XGD-SSP blends are shown in Figure 11. The peaks associated with the XGD polymer were identified at 3614, 1649, 1525, 1413, and 1029 cm^{-1} corresponding to the axial deformation of O-H; axial deformation of C-O ester, acid carboxylic, aldehydes, and ketones; axial deformation of C–O; axial deformation of C—O of enols; and deflection angle C–H(R. Ahmad & Mirza, 2018; Faria et al., 2011). The bands of MNS and SSP have been previously described.

a) b)

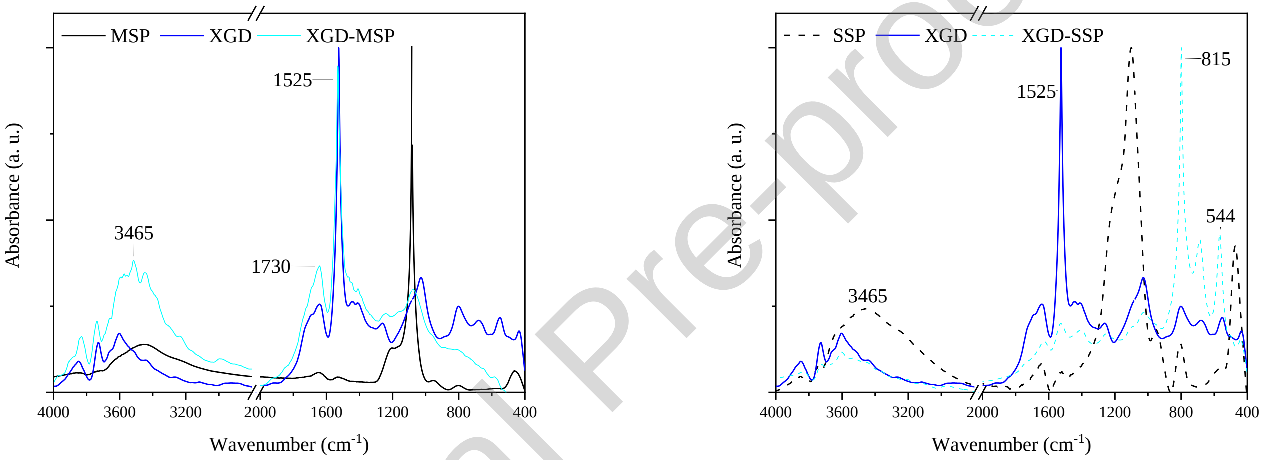

Figure 11. FTIR spectra of MSP, XGD, and XGD-MSP bled (a), and SSP, XGD, and XGD-SSP blend (b).

The spectra of the blends were a combination of the XGD and particles spectra. In general, significant changes are observed in the XGD-SSP spectra. The peaks at 3465 and 1085cm^{-1} in the blend decreased with respect to those in the SSP spectra. In addition, the signals at 815 and 544 cm^{-1} increased. The presence of peaks at 1085 and 815 cm^{-1} in the XGD-SSP spectrum indicated the formation of the XGD-SSP composite. In addition, the disappearance of some XGD peaks in the blend spectra indicates the participation of XGD in the formation of SSP (Al-Yasiri et al., 2019).

Overall, significant changes were observed in the spectra of blends containing SSP. Specifically, the peaks at 3465, 1656, 1085, and 466 cm^{-1} are associated with O–H stretching in H-bonded water, absorption of water molecules, superimposition of various SiO_2 peaks, Si–OH bonding, peaks due to residual organic groups, and tetrahedral bending modes of Si-OH-Si, respectively (Beganskienė et al., 2014). These changes could be related to the higher affinity of SSP for the BT, PAC, or XGD components, considering the physicochemical characteristics of SSP particles such as charge, size, and exposure of silanol groups. In previous studies, it was noted that these interactions were associated with a lack of increase in viscosity (Clavijo et al., 2019).

Filtration assays

The filtration properties are summarized in Table 1. Figure 12 shows the results obtained from the filtration assays conducted for 3-MSP and 3-SSP fluids. In the absence of NaCl (Figure 12a), the 3-MSP fluid exhibited a lower filtration volume than 3-SSP. Furthermore, it was observed that the filtration volume of 3-MSP increased with aging, converging to values similar to those of both 3-SSP and aged 3-SSP fluids. In the presence of NaCl, the filtration characteristics of the fluid changed with the type of particles employed (Figure 12b). In general, the presence of NaCl in fluids produces a decrease in the volume of filtrate for fluids containing particles improving the filtration properties. This observation can be attributed to the effect of salt on the surface interactions between the fluid components, which is enhanced at high temperatures promoting rearrangements in the filter cake structure.

a)

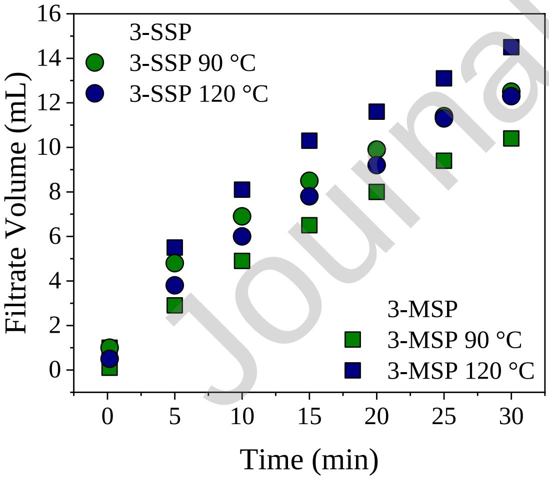

b)

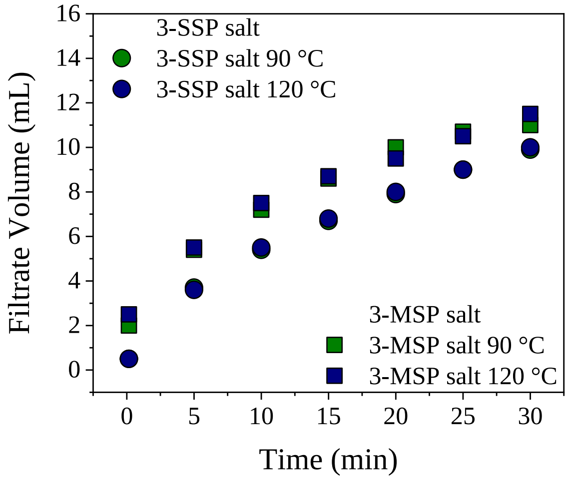

Figure 12. Filtration properties of 3-SSP and 3-MSP fluids (a) and 3-SSP and 3-MSP fluids with 0.75 M of NaCl (b).

The quality of the filter cake is the representative factor of the amount of filter loss, and in drilling operations, fluid loss should be prevented to guarantee wellbore stability. Therefore, this is one of the factors that should be addressed in drilling operations. To evaluate the filter cake performance, the filtrate volumes were measured for 30 min. The obtained cakes in both SSP- and MSP-based WBMs showed a homogeneous appearance with the absence of cracks (Figure 13a). Additionally, the filtrate volumes (Figure 13b) were similar and notably lower than the filtration volumes previously reported by our group for WBM without the addition of particles (less than 7 mL *vs* 14 mL) (Villada et al., 2022).

a) b)

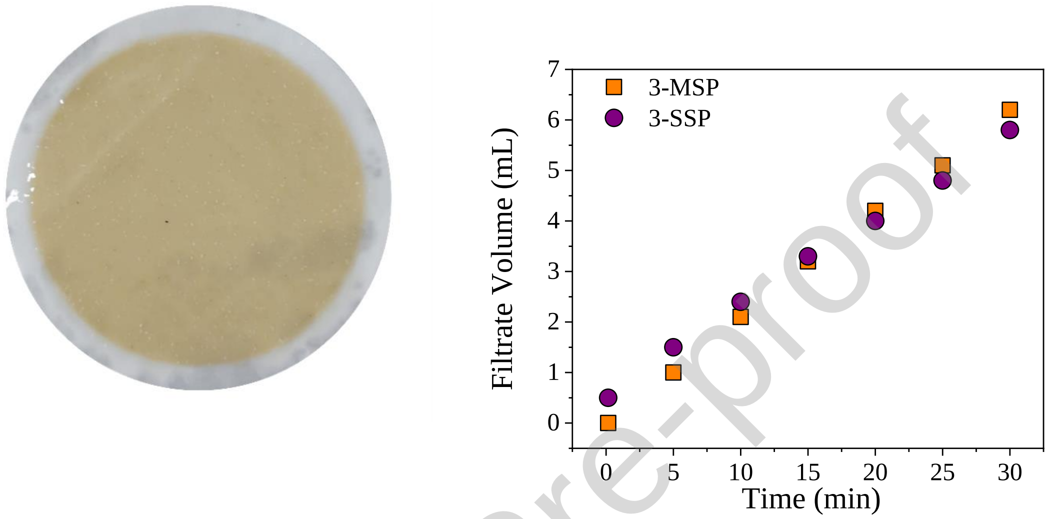

Figure 13. Picture of the 3-MSP filtration cake (a) and the performance of filter cakes obtained for 3-MSP and 3-SSP (b).

Conclusions

SSP and MSP particles with different characteristics (morphology, particle size, surface area, and charge) were synthesized and characterized, and their application as additives in the formulation of drilling fluids was studied. MSP particles have proven to be more effective as rheological modifiers, requiring lower concentrations (0.25% wt) to achieve comparable rheological properties to fluids containing SSPs. In addition, the ζ- potential showed that MSP exhibits better colloidal stability when combined with other components. However, SSP exhibited higher negative charges with BT, XGD, and PAC, associated with the changes in bands in the FTIR spectra and the ζ-potential values. Based on the results of the surface interactions, the rheological properties were mainly governed by surface interactions. In general, the WBMs based on MSP particles exhibited better filtration properties although its performance was enhanced in the presence of NaCl and temperature. On the other hand, a homogeneous distribution of the particles and particle aggregations was observed in the WBMs containing SSP and MSP, respectively.

Overall, the use of MSP as an additive in WBMs represents an attractive alternative for the academic and industrial areas because of its main physicochemical properties, such as surface area and morphology, and the required quantities that implicate a cost-effective benefit. The colloidal stability of the systems is affected by the interfacial properties, and it is expected a more stable suspension in the presence of other components (BT, XGD, and PAC). Likewise, the enhanced rheological properties of the drilling fluid contributed to its thermal stability. Also, the porous morphology of MSP could contribute positively to avoiding the blocking of the pore throat. Thus, to establish the viability of MSP in WBMs for industrial use, further investigations are necessary to experimentally study the surface interactions between components of WBMs and between the formation and WBMs in order to optimize its formulation and explore synergies between additives, and evaluate its long-term performance under realistic drilling conditions.

Acknowledgements

We acknowledge financial support from CONICET, MINCyT, and UNL.

Conflicts of Interest

The authors declare that they have no known competing financial interests or personal relationships that could have influenced the work reported in this study.

References

Afolabi, R. O. (2019). Enhanced oil recovery for emergent energy demand: challenges and prospects for a nanotechnology paradigm shift. *International Nano Letters*, *9*(1), 1–15. https://doi.org/10.1007/s40089-018-0248-0

Aftab, A., Ismail, A. R., Ibupoto, Z. H., Akeiber, H., & Malghani, M. G. K. (2017). Nanoparticles based drilling muds a solution to drill elevated temperature wells: A review. *Renewable and Sustainable Energy Reviews*, *76*(January), 1301–1313. https://doi.org/10.1016/j.rser.2017.03.050

Ahmad, H. M., Iqbal, T., A. Al Harthi, M., & Kamal, M. S. (2021). Synergistic effect of polymer and nanoparticles on shale hydration and swelling performance of drilling fluids. *Journal of Petroleum Science and Engineering*, *205*, 108763. https://doi.org/10.1016/j.petrol.2021.108763

Ahmad, R., & Mirza, A. (2018). Adsorptive removal of heavy metals and anionic dye from aqueous solution using novel Xanthan gum-Glutathione/ Zeolite bionanocomposite. *Groundwater for Sustainable Development*, *7*, 305–312. https://doi.org/10.1016/j.gsd.2018.07.002

Ali, I., Ahmad, M., & Ganat, T. (2022). Biopolymeric formulations for filtrate control applications in water-based drilling muds: A review. *Journal of Petroleum Science and Engineering*, *210*, 110021. https://doi.org/10.1016/j.petrol.2021.110021

Al-Yasiri, M., Awad, A., Pervaiz, S., & Wen, D. (2019). Influence of silica nanoparticles on the functionality of water-based drilling fluids. *Journal of Petroleum Science and Engineering*, *179*, 504–512. https://doi.org/10.1016/j.petrol.2019.04.081

Aramendiz, J., & Imqam, A. (2019). Water-based drilling fluid formulation using silica and graphene nanoparticles for unconventional shale applications. *Journal of Petroleum Science and Engineering*, *179*, 742–749. https://doi.org/10.1016/j.petrol.2019.04.085

Bardhan, A., Vats, S., Prajapati, D. K., Halari, D., Sharma, S., & Saxena, A. (2024). Utilization of mesoporous nano-silica as high-temperature water-based drilling fluids additive: Insights into the fluid loss reduction and shale stabilization potential. *Geoenergy Science and Engineering*, *232*, 212436. https://doi.org/10.1016/J.GEOEN.2023.212436

Bayat, A. E., & Shams, R. (2019). Appraising the impacts of SiO2, ZnO and TiO2 nanoparticles on rheological properties and shale inhibition of water-based drilling muds. *Colloids and Surfaces A: Physicochemical and Engineering Aspects*, *581*, 123792. https://doi.org/10.1016/j.colsurfa.2019.123792

Beganskienė, ldona, Sirutkaitis, V., Kurtrinaitienė, M., Juškėnas, R., & Kareiva, A. (2014). FTIR, TEM and NMR Iinvestigations of Stöber Silica Nanoparticles. *Material Science*, *10*(4).

Cai, Q., Luo, Z. S., Pang, W. Q., Fan, Y. W., Chen, X. H., & Cui, F. Z. (2001). Dilute solution routes to various controllable morphologies of MCM-41 silica with a basic medium. *Chemistry of Materials*, *13*(2), 258–263. https://doi.org/10.1021/cm990661z

Cao, L., Zhang, H., Cao, C., Zhang, J., Li, F., & Huang, Q. (2016). Quaternized Chitosan-Capped Mesoporous Silica Nanoparticles as Nanocarriers for Controlled Pesticide Release. *Nanomaterials 2016, Vol. 6, Page 126*, *6*(7), 126. https://doi.org/10.3390/NANO6070126

Cheraghian, G. (2021). Nanoparticles in drilling fluid: A review of the state-of-the-art. *Journal of Materials Research and Technology*, *13*, 737–753. https://doi.org/10.1016/j.jmrt.2021.04.089

Clavijo, J. V., Roldán, L. J., Valencia, L., Lopera, S. H., Zabala, R. D., Cárdenas, J. C., Durán, W., Franco, C. A., & Cortés, F. B. (2019). Influence of size and surface acidity of silica nanoparticles on inhibition of the formation damage by bentonite-free water-based drilling fluids. Part I: nanofluid design based on fluid-nanoparticle interaction. *Advances in Natural Sciences: Nanoscience and Nanotechnology*, *10*(4), 045020. https://doi.org/10.1088/2043-6254/ab5c17

Dankwa, O. K., Appau, P. O., & Broni-Bediako, E. (2018). Evaluating the Effects of Monovalent and Divalent Salts on the Rheological Properties of Water Based Mud. *The Open Petroleum Engineering Journal*, *11*(1), 98–106. https://doi.org/10.2174/1874834101811010098

Edalatfar, M., Yazdani, F., & Salehi, M. B. (2021). Synthesis and identification of ZnTiO3 nanoparticles as a rheology modifier additive in water-based drilling mud. *Journal of Petroleum Science and Engineering*, *201*, 108415. https://doi.org/10.1016/j.petrol.2021.108415

Esfandyari Bayat, A., Harati, S., & Kolivandi, H. (2021). Evaluation of rheological and filtration properties of a polymeric water-based drilling mud in presence of nano additives at various temperatures. *Colloids and Surfaces A: Physicochemical and Engineering Aspects*, *627*, 127128. https://doi.org/10.1016/J.COLSURFA.2021.127128

Fakoya, M. F., & Shah, S. N. (2017). Emergence of nanotechnology in the oil and gas industry: Emphasis on the application of silica nanoparticles. *Petroleum*, *3*(4), 391–405. https://doi.org/10.1016/j.petlm.2017.03.001

Faria, S., de Oliveira Petkowicz, C. L., de Morais, S. A. L., Terrones, M. G. H., de Resende, M. M., de França, F. P., & Cardoso, V. L. (2011). Characterization of xanthan gum produced from sugar cane broth. *Carbohydrate Polymers*, *86*(2), 469–476. https://doi.org/10.1016/j.carbpol.2011.04.063

Fookes, F., Busatto, C., Eugenia Taverna, M., Casis, N., Lescano, M., & Estenoz, D. (2022). Morphology modulation of silica mesoporous nano- and microparticles for atrazine - controlled release. *Environmental Nanotechnology, Monitoring & Management*, *18*, 100712. https://doi.org/10.1016/j.enmm.2022.100712

Gautam, S., Guria, C., & Rajak, V. K. (2022). A state of the art review on the performance of high-pressure and high-temperature drilling fluids: Towards understanding the structure-property relationship of drilling fluid additives. *Journal of Petroleum Science and Engineering*, *213*, 110318. https://doi.org/10.1016/j.petrol.2022.110318

Ibrahim, A. H., Smått, J.-H., Govardhanam, N. P., Ibrahim, H. M., Ismael, H. R., Afouna, M. I., Samy, A. M., & Rosenholm, J. M. (2020). Formulation and optimization of drug-loaded mesoporous silica nanoparticle-based tablets to improve the dissolution rate of the poorly water-soluble drug silymarin. *European Journal of Pharmaceutical Sciences*, *142*, 105103. https://doi.org/10.1016/j.ejps.2019.105103

Ikram, R., Jan, B. M., & Vejpravova, J. (2021). Towards recent tendencies in drilling fluids: application of carbon-based nanomaterials. *Journal of Materials Research and Technology*, *15*, 3733–3758. https://doi.org/10.1016/j.jmrt.2021.09.114

Islam, E., & Nebhani, L. (2021). Concerted effect of boron and porosity on shear thickening behavior of hybrid mesoporous silica dispersions. *Materials Today Chemistry*, *22*, 100565. https://doi.org/10.1016/j.mtchem.2021.100565

Kadhem, A., Xiang, S., Nagel, S., Lin, C.-H., & Fidalgo de Cortalezzi, M. (2018). Photonic Molecularly Imprinted Polymer Film for the Detection of Testosterone in Aqueous Samples. *Polymers*, *10*(4), 349. https://doi.org/10.3390/polym10040349

Karakosta, K., Mitropoulos, A. C., & Kyzas, G. Z. (2021). A review in nanopolymers for drilling fluids applications. *Journal of Molecular Structure*, *1227*, 129702. https://doi.org/10.1016/j.molstruc.2020.129702

Kennedy, J. R. M., Kent, K. E., & Brown, J. R. (2015). Rheology of dispersions of xanthan gum, locust bean gum and mixed biopolymer gel with silicon dioxide nanoparticles. *Materials Science and Engineering: C*, *48*, 347–353. https://doi.org/10.1016/j.msec.2014.12.040

Khalil, M., Amanda, A., Yunarti, R. T., Jan, B. M., & Irawan, S. (2020). Synthesis and application of mesoporous silica nanoparticles as gas migration control additive in oil and gas cement. *Journal of Petroleum Science and Engineering*, *195*, 107660. https://doi.org/10.1016/j.petrol.2020.107660

Kök, M. V., & Bal, B. (2019). Effects of silica nanoparticles on the performance of water-based drilling fluids. *Journal of Petroleum Science and Engineering*, *180*, 605–614. https://doi.org/10.1016/j.petrol.2019.05.069

Lagaly, G. (1989). Principles of flow of kaolin and bentonite dispersions. *Applied Clay Science*, *4*(2), 105–123. https://doi.org/10.1016/0169-1317(89)90003-3

Lavoine, N., Desloges, I., Dufresne, A., & Bras, J. (2012). Microfibrillated cellulose – Its barrier properties and applications in cellulosic materials: A review. *Carbohydrate Polymers*, *90*(2), 735–764. https://doi.org/10.1016/j.carbpol.2012.05.026

Li, M., Gu, S., Jin, J., Zheng, Y., & Xie, D. (2020). Research on the influence of polyanionic cellulose on the microstructure and properties of oil well cement. *Construction and Building Materials*, *259*, 119841. https://doi.org/10.1016/j.conbuildmat.2020.119841

Li, M.-C., Wu, Q., Song, K., French, A. D., Mei, C., & Lei, T. (2018). pH-Responsive Water-Based Drilling Fluids Containing Bentonite and Chitin Nanocrystals. *ACS Sustainable Chemistry & Engineering*, *6*(3), 3783–3795. https://doi.org/10.1021/acssuschemeng.7b04156

Liu, H., Jin, X., & Ding, B. (2016). Application of nanotechnology in petroleum exploration and development. *Petroleum Exploration and Development*, *43*(6), 1107–1115. https://doi.org/10.1016/S1876-3804(16)30129-X

Luckham, P. F., & Rossi, S. (1999). The colloidal and rheological properties of bentonite suspensions. *Advances in Colloid and Interface Science*, *82*(1–3), 43–92. https://doi.org/10.1016/S0001-8686(99)00005-6

Mirzaasadi, M., Zarei, V., Elveny, M., Alizadeh, S. M., Alizadeh, V., & Khan, A. (2021). Improving the rheological properties and thermal stability of water-based drilling fluid using biogenic silica nanoparticles. *Energy Reports*, *7*, 6162–6171. https://doi.org/10.1016/j.egyr.2021.08.130

Narayan, R., Nayak, U., Raichur, A., & Garg, S. (2018). Mesoporous Silica Nanoparticles: A Comprehensive Review on Synthesis and Recent Advances. *Pharmaceutics*, *10*(3), 118. https://doi.org/10.3390/pharmaceutics10030118

Novara, R., Rafati, R., & Sharifi Haddad, A. (2021). Rheological and filtration property evaluations of the nano-based muds for drilling applications in low temperature environments. *Colloids and Surfaces A: Physicochemical and Engineering Aspects*, *622*, 126632. https://doi.org/10.1016/j.colsurfa.2021.126632

Porgham Daryasari, M., Dusti Telgerd, M., Hossein Karami, M., Zandi-Karimi, A., Akbarijavar, H., Khoobi, M., Seyedjafari, E., Birhanu, G., Khosravian, P., & SadatMahdavi, F. (2019). Poly-l-lactic acid scaffold incorporated chitosan-coated mesoporous silica nanoparticles as pH-sensitive composite for enhanced osteogenic differentiation of human adipose tissue stem cells by dexamethasone delivery. *Artificial Cells, Nanomedicine and Biotechnology*, *47*(1), 4020–4029. https://doi.org/10.1080/21691401.2019.1658594

Rafati, R., Smith, S. R., Sharifi Haddad, A., Novara, R., & Hamidi, H. (2018). Effect of nanoparticles on the modifications of drilling fluids properties: A review of recent advances. *Journal of Petroleum Science and Engineering*, *161*(December 2017), 61–76. https://doi.org/10.1016/j.petrol.2017.11.067

Salih, A. H., Elshehabi, T. A., & Bilgesu, H. I. (2016, September 13). Impact of Nanomaterials on the Rheological and Filtration Properties of Water-Based Drilling Fluids. *All Days*. https://doi.org/10.2118/184067-MS

Scheid, C. M., de Carvalho, R. V., de Oliveira, B. R., de Oliveira Borges, R. F., & Calçada, L. A. (2019). Evaluation of the dissolution kinetics of NaCl particles in aqueous drilling fluids viscosified with bentonite. *Journal of Petroleum Science and Engineering*, *174*, 563–571. https://doi.org/10.1016/j.petrol.2018.11.017

Shnoudeh, A. J., Hamad, I., Abdo, R. W., Qadumii, L., Jaber, A. Y., Surchi, H. S., & Alkelany, S. Z. (2019). Synthesis, Characterization, and Applications of Metal Nanoparticles. *Biomaterials and Bionanotechnology*, 527–612. https://doi.org/10.1016/B978-0-12-814427-5.00015-9

Sun, J., Chang, X., Lv, K., Wang, J., Zhang, F., Jin, J., Zhou, X., & Dai, Z. (2021). Environmentally friendly and salt-responsive polymer brush based on lignin nanoparticle as fluid-loss additive in water-based drilling fluids. *Colloids and Surfaces A: Physicochemical and Engineering Aspects*, *621*, 126482. https://doi.org/10.1016/j.colsurfa.2021.126482

Vallet-Regí, M. (2022). Our contributions to applications of mesoporous silica nanoparticles. *Acta Biomaterialia*, *137*, 44–52. https://doi.org/10.1016/j.actbio.2021.10.011

Villada, Y., Busatto, C., Casis, N., & Estenoz, D. (2022). Use of synthetic calcium carbonate particles as an additive in water-based drilling fluids. *Colloids and Surfaces A: Physicochemical and Engineering Aspects*, *652*, 129801. https://doi.org/10.1016/j.colsurfa.2022.129801

Villada, Y., Gallardo, F., Erdmann, E., Casis, N., Olivares, L., & Estenoz, D. (2017). Functional characterization on colloidal suspensions containing xanthan gum (XGD) and polyanionic cellulose (PAC) used in drilling fluids for a shale formation. *Applied Clay Science*, *149*, 59–66. https://doi.org/10.1016/j.clay.2017.08.020

Villada, Y., Iglesias, M. C., Casis, N., Erdmann, E., Peresin, M. S., & Estenoz, D. (2018). Cellulose nanofibrils as a replacement for xanthan gum (XGD) in water based muds (WBMs) to be used in shale formations. *Cellulose*, *25*(12), 7091–7112. https://doi.org/10.1007/s10570-018-2081-z

Villada, Y., Iglesias, M. C., Olivares, M. L., Casis, N., Zhu, J., Peresin, M. S., & Estenoz, D. (2020). Di-carboxylic acid cellulose nanofibril (DCA-CNF) as an additive in water-based drilling fluids (WBMs) applied to shale formations. *Cellulose*, *28*(1), 417–436. https://doi.org/10.1007/s10570-020-03502-1

Vryzas, Z., & Kelessidis, V. C. (2017). Nano-based drilling fluids: A review. *Energies*, *10*(4). https://doi.org/10.3390/en10040540

Vryzas, Z., Nalbandian, L., Zaspalis, V. T., & Kelessidis, V. C. (2019). How different nanoparticles affect the rheological properties of aqueous Wyoming sodium bentonite suspensions. *Journal of Petroleum Science and Engineering*, *173*, 941–954. https://doi.org/10.1016/j.petrol.2018.10.099

William, J. K. M., Ponmani, S., Samuel, R., Nagarajan, R., & Sangwai, J. S. (2014). Effect of CuO and ZnO nanofluids in xanthan gum on thermal, electrical and high pressure rheology of water-based drilling fluids. *Journal of Petroleum Science and Engineering*, *117*, 15–27. https://doi.org/10.1016/j.petrol.2014.03.005

Williams, S., Neumann, A., Bremer, I., Su, Y., Dräger, G., Kasper, C., & Behrens, P. (2015). Nanoporous silica nanoparticles as biomaterials: evaluation of different strategies for the functionalization with polysialic acid by step-by-step cytocompatibility testing. *Journal of*

Materials Science: Materials in Medicine, *26*(3). https://doi.org/10.1007/s10856-015-5409-3

Yang, H., Deng, Y., Du, C., & Jin, S. (2010). Novel synthesis of ordered mesoporous materials Al-MCM-41 from bentonite. *Applied Clay Science*, *47*(3–4), 351–355. https://doi.org/10.1016/j.clay.2009.11.050

Zarei, V., Yavari, H., Nasiri, A., Mirzaasadi, M., & Davarpanah, A. (2023). Implementation of Amorphous Mesoporous Silica Nanoparticles to formulate a novel water-based drilling fluid. *Arabian Journal of Chemistry*, *16*(8), 104818. https://doi.org/10.1016/J.ARABJC.2023.104818

Declaration of Competing Interest

☒ The authors declare that they have no known competing financial interests or personal relationships that could have appeared to influence the work reported in this paper.

☐ The authors declare the following financial interests/personal relationships which may be considered as potential competing interests:

Highlights

- The effect of silica particles type on water-based drilling fluids (WBMs) performance was investigated.
- Lower concentrations of mesoporous silica particles (MSP) were required to achieve the same rheological properties of the fluids containing non-porous silica particles (SSP).
- The physicochemical properties of SSP and MSP such as size, morphology, and surface charge had a different effect on the performance of WBMs.
- The surface interactions mainly governed the rheological properties of WBMs.